Measuring Hydrate/Ice Deposition in a Flow Loop from Dissolved Water in Live Liquid Condensate

Joseph W. Nicholas, Carolyn A. Koh, and E. Dendy Sloan
Chemical Engineering Dept., Colorado School of Mines, Golden, CO 80401

Lee Nuebling and Helen He
Intertek Westport Technology Center, Houston, TX 77024

Bob Horn
RAB Co., Montgomery, TX 77356

DOI 10.1002/aic.11874
Published online May 28, 2009 in Wiley InterScience (www.interscience.wiley.com).

Experiments were conducted to investigate hydrate/ice plugging and deposition mechanisms from water dissolved in a liquid condensate system, using a single-pass flow loop. Two different hydrate/ice plugging mechanisms were observed. Hydrate/ice deposition from a dissolved-water phase resulted in a lengthwise uniform/dispersed deposit and a gradual pressure drop increase. The dispersed deposit acted as insulation at the flow loop wall, and the deposit began to propagate downstream. However, cooling below the liquid-water saturation curve resulted in free water coalescence, and a localized hydrate/ice restriction in the flow loop. This localized restriction resulted in a rapid pressure drop increase. © 2009 American Institute of Chemical Engineers *AIChE J,* 55: 1882–1888, 2009

Keywords: hydrate, ice, deposition, plugging, flow loop

Introduction

Clathrate hydrates have hindered the oil and gas industry since 1934, when Hammerschmidt discovered hydrates were capable of plugging pipelines.[1] Clathrate hydrates are crystalline inclusion compounds wherein hydrogen-bonded water molecules form cages containing guest molecules.[2] Hydrates form at high-pressures and low-temperatures, similar to conditions in flow lines on the sea floor. Because hydrocarbons act as guest molecules, offshore pipelines are prime candidates for hydrate formation and plugging. In addition to lost production and revenue, hydrates pose a significant safety hazard, due to gas expansion upon heating, or projectile-like properties when dislodged.[3]

In 1994 Lingelem et al. suggested that hydrates formed in condensate pipelines deposit on the pipe wall, similar to a freezing water pipeline.[4] Two prolific hydrate field studies conducted in both the Werner Bolley[5] and Tommeliten Gamma[6] fields suggest hydrates may have adhered to the pipe wall. Both tests observed pressure buildups and falloffs that would be consistent with hydrate deposits on the pipe wall before sloughing downstream to form a plug. However, there is still a debate within the oil and gas industry as to whether or not hydrate deposition occurs in pipelines.[7,8] This work investigated the feasibility of hydrate/ice deposition in a single-pass flow loop using a water saturated liquid condensate.

Predicting hydrate formation and deposition in water saturated systems has a direct application to gas export and sales

Correspondence concerning this article should be addressed to J. W. Nicholas joe.nicholas@meritenergy.com or E. Dendy Sloan at esloan@mines.edu.
Current address of J. W. Nicholas, Merit Energy, 13727 Noel Road, Suite 500, Dallas, TX 75240.

pipelines. Before entering these lines, gas is dehydrated to field specifications; however, occasionally these specifications still result in hydrate formation.[9] This scenario becomes exacerbated when flow line conditions fluctuate with ambient temperatures, as is the case in many onshore pipelines. Gas export and sales lines affected by seasonal temperatures include: arctic pipelines, residential pipelines, and other lines exposed to harsh winters.

Hydrate blockages are typically removed via depressurization; however, at temperatures below the ice point, hydrate blockages convert to ice upon depressurization. Once an ice plug is formed it becomes very difficult to remove and may even lead to pipeline abandonment. Arctic pipelines, such as an Alaskan or Canadian sales line, are of particular interest to this work, because the ambient temperatures in those regions are often below freezing. This work measured the consequences of operating within the hydrate formation region, which may occur during a seasonal cool down or a dehydrator malfunction.

Figure 2. Picture of test section which was comprised of 14 heat exchangers.

[Color figure can be viewed in the online issue, which is available at www.interscience.wiley.com.]

Experimental Apparatus and Procedure

Figure 1 shows an illustration of the single-pass flow loop used in these experiments. The flowloop was constructed at Intertek Westport Technology Center in Houston, TX. Figure 1 shows the flow loop consisted of a cooling section, test section, and reheat section. The cooling and reheat sections were each 18.2 m in length, while the test section was 85.3 m in length. The flow loop was constructed using a series of 6.1 m long, coiled, pipe-in-pipe heat exchangers with an inner diameter of 9.3 mm. A picture of the 85.3 m test section is shown in Figure 2.

Pressure and temperature profiles were measured every minute between each of the 12.2 m sections. Water concentrations were measured before the cooling section and after the reheat section using General Electric M series moisture probes with an absolute accuracy of ± 30%.[10] After establishing the probes baseline reading in each experiment, the probes could be reliably used for detecting relative change in moisture content.[7] Moisture content was maintained throughout the course of the experiment using an ultrasonic mixing system upstream of the separator.

Pressure was measured using Heise PM1 dual pressure transducers with an accuracy of ± 0.025% and Omega K series dual thermocouples were used to monitor temperature with an accuracy of ± 1°C. Flow rate was measured using a Blancett 1200 turbine flow meter with an accuracy of ± 1%. All flow loop instrumentation was factory calibrated. Detailed information concerning the flow loop design, instrumentation, and commissioning procedures are documented in Nicholas' thesis.[7]

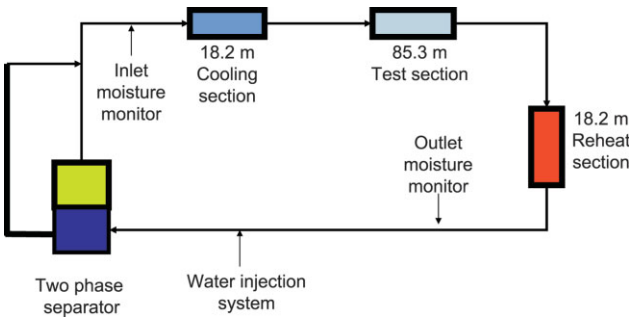

Figure 1. Illustration of single-pass flow loop.

[Color figure can be viewed in the online issue, which is available at www.interscience.wiley.com.]

All experiments were conducted with an industrial condensate detailed in Table 1. The condensate was then mixed with 3.5 wt % propane and pressurized to 6.89 MPa with commercial grade methane. Experiments were performed at 100% liquid loading, using only the liquid stream from the separator. Experimental temperatures were designed to

Table 1. Experimental Condensate Composition

Component	Weight percent
i-C4	0.03
n-C4	0.12
Neopentane	0.43
i-C5	13.25
n-C5	12.68
2,2-Dimethylbutane	1.10
N-hexane	8.35
Fractional C6	16.51
Methylcyclopentane	4.58
Benzene	3.27
Cyclohexane	5.74
N-heptane	4.35
Fractional C7	9.82
Methylcyclohexane	6.01
Toluene	2.87
n-C8	1.45
Fractional C8	4.53
Ethylbenzene	0.2
mp-xylene	0.8
o-xylene	0.18
Fractional C9	1.94
C10	0.47
C11	0.18
C12	0.05
Total	98.91

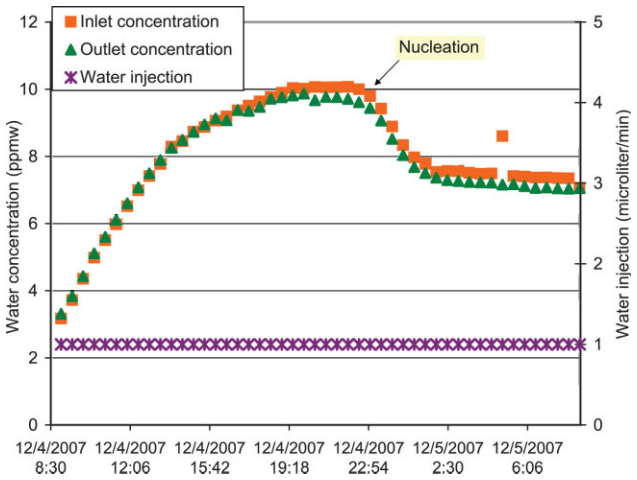

Figure 3. Water concentrations and injection rates throughout solid nucleation on the flow loop wall.

[Color figure can be viewed in the online issue, which is available at www.interscience.wiley.com.]

simulate arctic conditions and ranged from −21°C to 3°C. Condensate flow rates were limited by the pump speed and maintained at either 1.89 L/min (~0.3 m/s), or 2.83 L/min (~0.6 m/s).

Experimental Results and Discussion

Experiments were performed to investigate the following behavior: solid nucleation, equilibrium concentrations, plugging mechanisms, long-term deposition, and solid dissociation. A total of six experiments ranging from 1–3 weeks were conducted on this apparatus.[7] Because each experiment consisted of multiple investigations, only the key experimental results are discussed.

INFOCHEM's Multi-Flash was used to predict water saturation concentrations for the live condensate described in Table 1. These predictions were used in explaining and validating the subsequent experimental results. Before these predictions, Multi-Flash was benchmarked against water saturation concentrations in n-decane; whereby Multi-Flash was found to match the predictive correlations provided by Tsnopoulos.[12]

Nucleation

Nucleation metastability at −21°C and 2.83 L/min was probed by injecting water at rate of 1 mL/min until hydrate/ice nucleated. Figure 3 shows the water concentration in the condensate increased as water was slowly injected into the flow loop. The inflection at 12/4/07 13:00 suggests nucleation may have initiated at approximately 8 ppmw. However, after reaching a condensate water concentration of 9–10 parts per million by weight (ppmw) at 12/4/07 23:00, the water concentration rapidly decreased to the equilibrium concentration of 7 ppmw. This rapid decrease in moisture content confirmed that hydrate/ice had nucleated on the pipe wall, leaving the condensate water concentration in equilibrium with the hydrate/ice on the pipe wall as the fluid flowed past the solid deposit. Because the test section temperature was below 0°C and no direct measurements were made, it was not possible to distinguish between ice and hydrate in this experiment. Figure 3 demonstrates that a water concentration driving force of ~1–3 ppmw was required to nucleate hydrate/ice on the flow loop wall.

Equilibrium measurements

Equilibrium water concentrations at various temperatures were measured by completing a cooling and reheating loop as illustrated in Figure 4a. Figure 4a shows water content decreased with temperature from 15 to 0°C which was due to water adsorbing to the flow loop wall.[7] Water vapor is known to adsorb to stainless steel surfaces,[13] and these adsorption layers are expected to increase with decreasing temperature, analogous to other adsorption phenomena.

However, shortly after 0°C an inflection point was observed, which was believed to be the formation of ice. Upon reheating, it can be observed that the water concentrations remained below the cooling curve until reaching an

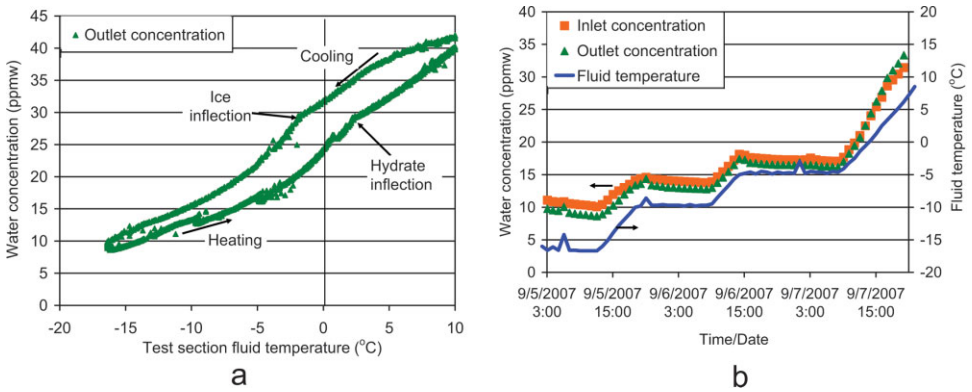

Figure 4. Water concentration profiles during the equilibrium measurements (a) water concentration vs. temperature throughout the cooling and reheating curve, and (b) water concentration and temperature profiles during the heating portion of Figure 4a.

[Color figure can be viewed in the online issue, which is available at www.interscience.wiley.com.]

Table 2. Experimental Equilibrium Measurements Compared with INFOCHEM Multi-Flash Predictions Using the CPA Model[11]

T (°C)	Flowloop Measurments (ppmw)	Multi-Flash CPA Ice Predictions (ppmw)	Mulit-Flash CPA Hydrate Predictions (ppmw)
−16.7	9.5±2.1	8.5	6.3
−9.7	13.5±4.1	19.7	15.9
−4.7	17±5.1	27.9	22.5

inflection point at 2.5°C. The combination of: (1) the hysteresis of this profile, and (2) the evidence of inflection points at 0°C and 2.6°C, suggest a metastable ice phase initially formed and converted to the equilibrium hydrate phase as the system was heated.

Figure 4b shows the water concentration and temperature profiles during the temperature ramp illustrated in Figure 4a. After the water content stabilized at −16.7°C, the temperature was increased at a rate of 1°C/h. Eight to 10 hour stops were held at −9.7°C and −4.7°C before proceeding to 15°C at a rate of 1°/h. Figure 4b shows the moisture content stabilized within 1- 2 ppmw at each temperature isotherm plateau (−16.7°C, −9.7°C, −4.7°C). These plateaus represent the condensate water concentration in equilibrium with either ice/hydrate. In addition to the condensate maintaining a constant water concentration during each eight to 10 h stop, the measurements were also corroborated by equilibrium predictions using INFOCHEM's Multi-Flash[11] software as shown in Table 2. Although the inflection point in Figure 4a indicates hydrates were present, this was not directly confirmed.

Plugging mechanisms

Prior to this work, it was unknown whether hydrates would deposit on the pipe wall or form as small particles and be transported in fluid flow. Plugging and deposition mechanisms were tested by operating the cooling and test sections at 3.7°C ± 0.3°C and 1.2°C ± 0.5°C, respectively. Flow rate was maintained at 1.89 L/min.

Figure 5 shows the flow loop operation at equilibrium conditions (30 ppmw) before water injection at 10/1/07 12:00. Upon water injection, the inlet concentration increased 12 ppmw to 42 ppmw. Meanwhile, the outlet concentration did not increase, indicating water deposited as hydrate on the flow loop wall and the water concentration decreased to the equilibrium concentration before exiting the test section. The pressure drop profile illustrated in Figure 5 indicates hydrates deposited in the cooling section. The cause of the sudden decrease and increase in the outlet concentration reading at 10/1/07 12:00 and 10/2/07 14:00 was likely due to an operating error.[7]

A gradual pressure drop increase was observed at the beginning of the experiment, which was then followed by a rapid pressure drop increase at 10/3/07 12:00. The gradual increase in pressure drop occurred when the inlet concentration was lower than the liquid water saturation concentration. This condition resulted in hydrate deposits on the pipe wall from the dissolved water phase, yielding a lengthwise dispersed solid deposit. The rapid increase in pressure drop at 10/3/07 12:00 resulted from the inlet water concentration

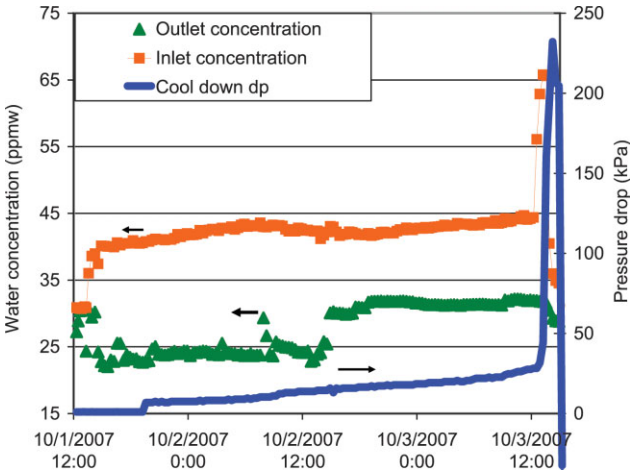

Figure 5. Water concentration and pressure-drop profiles while investigating the plugging/deposition mechanism.

[Color figure can be viewed in the online issue, which is available at www.interscience.wiley.com.]

exceeding the predicted liquid water-condensate single-phase limit, 46 ppmw, at 3.7°C.[11] Figure 5 shows this behavior to be coincident with increasing the inlet water concentration to 65 ppmw.

In contrast to the lengthwise uniform deposition over an extended length of flow loop ($\Delta P < 6.89$ kPa/h), the rapid pressure increase ($\Delta P > 6.89$ kPa/h) in Figure 5 likely resulted from the coalescence of free water, which then quickly converted to hydrate, and formed a localized restriction in the initial section of the flow loop.

Figure 6 illustrates the hypothesized plugging mechanisms on a phase diagram. Hydrate deposition from a dissolved water phase is depicted by the arrow at 42 ppmw. As the

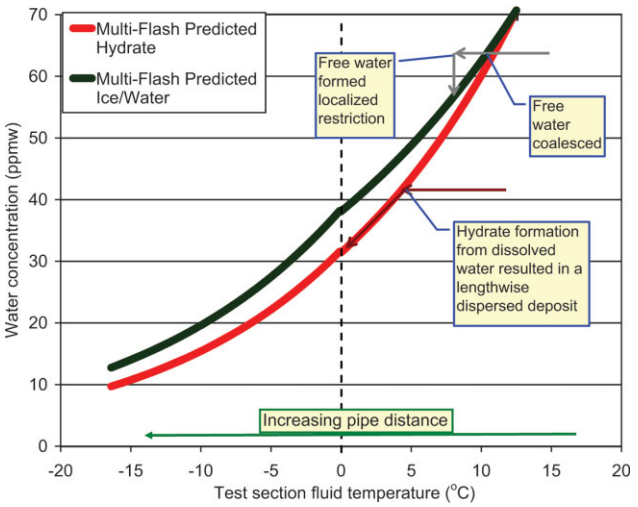

Figure 6. Illustration of hydrate formation from a free-water phase and a dissolved-water phase.

Ice/water and hydrate equilibrium water concentrations at 1,000 psia were predicted using INFOCHEM Multi-Flash with the CPA model.[11] [Color figure can be viewed in the online issue, which is available at www.interscience.wiley.com.]

fluid cools, hydrate formation conditions are encountered and water is incrementally removed from condensate to the hydrate deposit as fluid moves downstream and continues to cool. Upon increasing the inlet concentration to 65 ppmw, the condensate stream crossed both the hydrate and liquid water saturation curve, resulting in a free-water phase. This free-water phase then quickly formed a localized hydrate deposit, similar to an orifice restriction, in contrast to the dispersed lengthwise deposit from the dissolved-water phase.

In a separate experiment conducted at −21°C and 1.89 L/min, an attempt was made to reproduce the rapid pressure drop after nucleation had occurred. Figure 7 shows that water concentration was increased to as high as 50 ppmw, which was expected to provide free water as the condensate was cooled in the test section. However, as shown by the gradual pressure drop increase in Figure 7, hydrate/ice deposition appears to have formed from the dissolved-water phase.

Figure 8 illustrates a hypothesis to explain why a rapid pressure drop was not always observed when the inlet water concentration was above the liquid-water saturation concentration at 0°C. Figure 8 shows that the presence or absence of existing hydrate on the pipe wall played a critical role in determining the type of plugging mechanism. In the case where hydrates were not on the pipe wall, the inlet water concentration (C_w) remained constant until the condensate was cooled below the liquid water saturation curve. At the test section length where the condensate was cooled below saturation, free water dropped out of solution, creating a localized restriction.

However, if hydrates were present on the pipe wall, water was incrementally removed from the condensate to the hydrate deposit as the mixture flowed downstream, past the deposit. The water content of the condensate was likely in equilibrium with hydrate as it moved downstream, preventing the condensate water content from crossing the liquid-water saturation line, and resulting in lengthwise uniform/dispersed deposition.

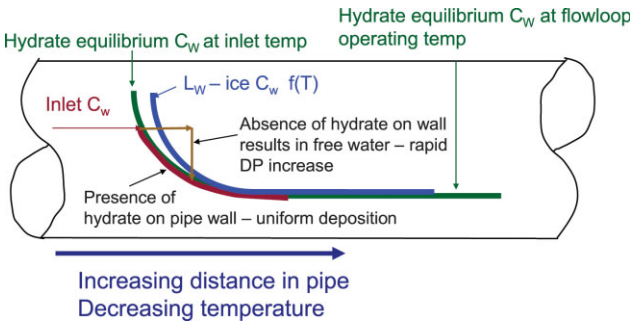

Figure 8. Hypothesized conceptual picture describing rapid pressure drop increase and uniform/dispersed deposition.

The various inlet and equilibrium water concentrations (C_w) are shown. Fluid temperature decreases as it flows downstream, resulting in lower equilibrium concentrations for both the hydrate and liquid water (L_w)/ice saturation curves. [Color figure can be viewed in the online issue, which is available at www.interscience.wiley.com.]

Long-term deposition experiment

A long-term deposition test was conducted at −21°C and a flow rate of 2.83 L/min as illustrated in Figure 9. After hydrate/ice nucleated, the water injection was increased at 8:00 on 12/5/07, which resulted in an inlet concentration of 24 ppmw. The inlet concentration was held at approximately 23–25 ppmw, while the outlet concentration remained at the equilibrium concentration of 7 ppmw. The difference in concentrations indicated that solids deposited in the flow loop test section as hydrate or ice, resulting in the shown pressure drop increase. The sudden decrease in outlet concentration at 12/9/07 6:30 in Figure 9 was a result of a probe error.[7]

Figure 10 illustrates the pressure drop profiles throughout the initial portions of the test section. Each pressure-drop in Figure 10 curve represents pressure drop between the test

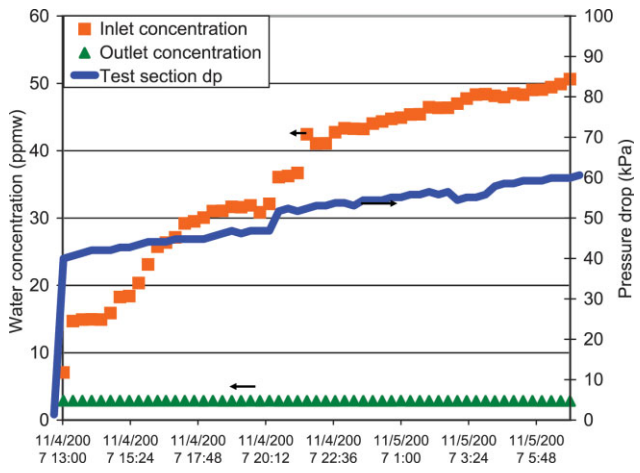

Figure 7. Water concentration and pressure-drop profiles while attempting to repeat rapid pressure drop increase.

[Color figure can be viewed in the online issue, which is available at www.interscience.wiley.com.]

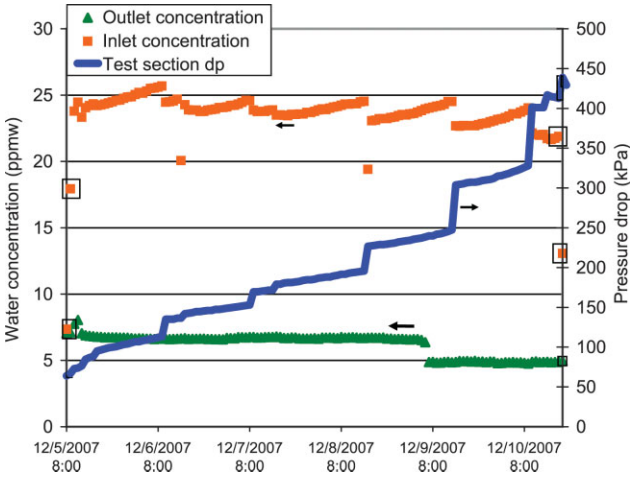

Figure 9. Water concentration profiles and resulting test section pressure-drop profile throughout long-term deposition experiment.

[Color figure can be viewed in the online issue, which is available at www.interscience.wiley.com.]

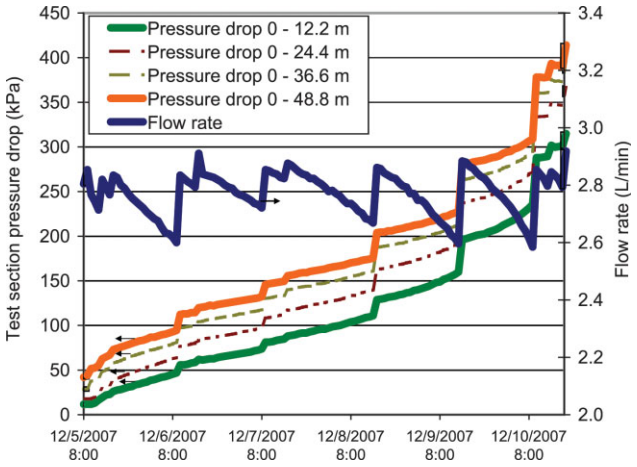

Figure 10. Flow rate and test section pressure-drop profiles during the uniform/dispersed deposition testing.

Each of the pressure drop profiles represents pressure drop across an additional 12.2 m in the test section. [Color figure can be viewed in the online issue, which is available at www.interscience.wiley.com.]

section inlet and an additional 12.2 m. Step changes in the test section pressure drop resulted from manually increasing pump speed to maintain a constant flow rate. Initially the 0–12.2 m pressure-drop curve in Figure 10 began to increase, while the distance between the remaining curves remained constant, indicating hydrate/ice was building up in the first 12.2 m of test section. Because flow rate decreased with increasing pressure drop, the pump speed was manually adjusted to maintain the target flow rate. Thus, it is necessary to compare pressure drops at similar flow rates.

At approximately 12/6/07 8:00 the two bottom curves started to diverge (0–12.2 m and 0–24.4 m) indicating the initiation of hydrate deposits between 12.2 m and 24.4 m in the test section. This behavior occurred because the hydrate/

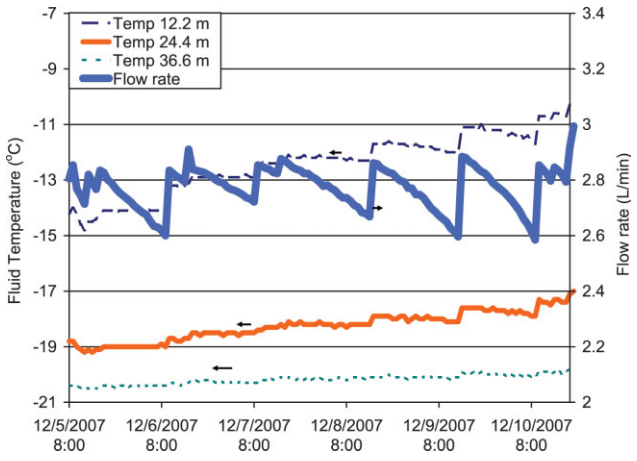

Figure 11. Flow rate and test section temperature profiles during uniform/dispersed deposition testing.

[Color figure can be viewed in the online issue, which is available at www.interscience.wiley.com.]

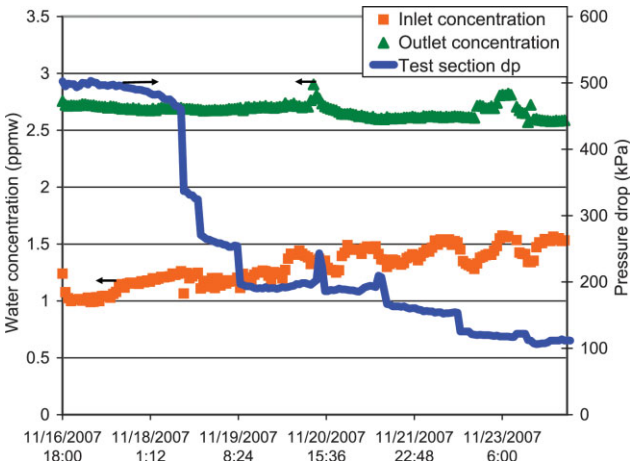

Figure 12. Water concentration and test section pressure drop while running the condensate through a molecular sieve unit.

[Color figure can be viewed in the online issue, which is available at www.interscience.wiley.com.]

ice deposit at the beginning of the test section (within 12.2 m) acted as insulation, and resulted in a fluid temperature increase throughout the first 12.2 m of the test section.

Figure 11 shows the temperature 12.2 m into the test section gradually increased as hydrate/ice deposited in the flow loop and acted as insulation. Similar to the pressure-drop profiles, it is important to compare the temperature profiles at similar flow rates. Figure 11 also confirms that hydrate/ice was depositing between 12.2 m and 24.4 m; in addition there was slight deposition between 24.4 m and 36.6 m.

A uniform/dispersed deposition experiment was conducted immediately after solid nucleation at −21°C, 6.89 MPa and

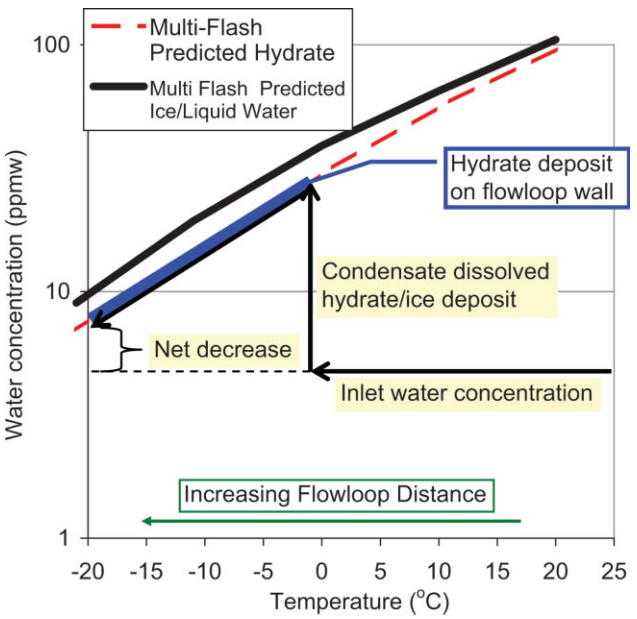

Figure 13. Illustration of an undersaturated condensate stream dissociating the hydrate/ice deposit.

[Color figure can be viewed in the online issue, which is available at www.interscience.wiley.com.]

a loop flow rate of 2.83 L/min. The inlet water concentration was maintained between 23–25 ppmw, while the outlet concentration remained at 7 ppmw. The solid accumulation on the pipe walls resulted in a pressure drop increase, across the first 48.8 m of the test section, from approximately 40 kPa to 400 kPa over the course of five days. The majority of the hydrate deposited in the first 24.4 m of the test section, which also resulted in an increase in condensate temperature throughout those sections.

Dissociation

The final area of investigation was to dissociate a hydrate/ice deposit that was formed at −21°C and 1.89 L/min, using a molecular sieve dehydrator. Following a two-week deposition test,[7] water injection was stopped and condensate was routed through a molecular sieve unit located between the reheat section and the separator, so that the inlet water concentration of the condensate was reduced to 1–1.5 ppmw.

Figure 12 shows the inlet concentration dropped below the outlet concentration after the dehydrator was installed at 11/16/07 16:15. Consequently, water was removed from the test section and pressure drop decreased. An illustration of this phenomenon is shown in Figure 13. The undersaturated condensate stream was cooled as it passed through the flow loop. Upon contacting the hydrate/ice deposit, the condensate stream dissolved the solid deposit until the condensate water concentration was in equilibrium with the solid deposit. As the stream was further cooled, a portion of the dissolved water was redistributed as hydrate/ice further downstream in the flow loop.[11] However, as illustrated in Figure 13, there is still a net decrease in water within the flow loop, supporting the dissociation of hydrate. The fact that the discharge water concentration remained constant throughout the dissociation experiment (Figure 12), suggests that all the hydrate/ice deposit was not removed in the test section. This experiment successfully proved the concept of dissociating a hydrate deposit with an undersaturated fluid.

Conclusions

Experiments were conducted to investigate hydrate/ice plugging and deposition mechanisms in a water saturated liquid condensate system, using a single-pass flow loop. Hydrate/ice was nucleated with a driving force of ∼3 ppmw and equilibrium measurements were completed by monitoring the condensate water concentrations. Water concentrations in equilibrium with hydrate or ice were indistinguishable below 0°C. However, solid-liquid-water equilibrium concentrations were measured using the flow loop outlet concentration.

Two different hydrate/ice plugging mechanisms were observed:

1. A rapid pressure drop increase (>6.89 kPa/h) was observed when the condensate was cooled below the liquid water saturation curve. Crossing the liquid water saturation curve resulted in free-water coalescing and forming a localized hydrate/ice restriction in the flow loop.

2. Uniform/dispersed deposition from a dissolved water phase resulted in a slow pressure drop increase (<6.89 kPa/h) throughout the first 12.2–24.4 m of the flow loop. During uniform/dispersed deposition it was found that the hydrate/ice deposit acted as insulation on the pipe wall, resulting in the solid deposit propagating downstream.

The uniform hydrate/ice deposits were removed by dehydrating the inlet condensate stream. Dehydrating the condensate stream reduced the inlet water concentration below the two-phase equilibrium concentration, while the outlet concentration remained at the equilibrium concentration. This behavior was accompanied by a decrease in pressure drop as water was removed from the test section.

Acknowledgements

This work was supported by Imperial Oil Limited, ExxonMobil, ConocoPhillips, and Shell. The authors gratefully acknowledge advice and support from: Alex Watson, Glenn Cobb, Larry Talley, Doug Turner, David Peters, Greg Hatton, Dan Crosby, Aftab Khokhar, Nick Wolf, and Tom Baugh.

Literature Cited

1. Hammerschmidt EG. Formation of gas hydrates in natural gas transmission lines. *Ind Eng Chem.* 1934;26(8):851–855.
2. Sloan ED, Koh CA. *Clathrate Hydrates of Natural Gases*. 3rd ed., New York: Taylor and Francis Group, LLC; 2008.
3. Sloan ED. *Hydrate Engineering*. Richardson, TX; 2000.
4. Lingelem MN, Majeed AI, Stange E. *Industrial Experience in Evaluation of Hydrate Formation, Inhibition and Dissociation in Pipeline Design and Operation.* Sloan ED, Happel J, Hnatow MA, eds. *International Conferance on Natural Gas Hydrates*, NYAS. 1994;715:75.
5. Hatton GJ, Klomp UC, Mehta AP. Personal Communication with Shell. December 2, 2005.
6. Austvik T, Hustvedt E, Meland B, Berge LI, Lysne D. Tommeliten Gamma Field Hydrate Experiments. *7th BHRA International Conferance on Multiphase Flow, Pblctn 14, Cnnes, FR 6/7-9/95.* 1995:539.
7. Nicholas JW. Hydrate Deposition in Water Saturated Liquid Condensate Systems. Colorado School of Mines, Golden, CO; 2008. PhD Thesis.
8. Matthews P, Creek J, Ballard A, Rhyne L, Talley L, Hernandez OC, Koh C, Sloan ED, Chitwood J. Personal communication - Discussing a Gas Dominated Hydrate Plugging Model. In Houston, TX; February 6, 2006.
9. Kane M, Singh A, Hanssen R. *Hydrates Blockage Experience in a Deep Water Subsea Dry Gas Pipeline: Lessons Learned,* Offshore Technology Conference, Houston, TX, May 5–8, 2008, Houston, TX; 2008.
10. Ardis M. Personal communication with GE Applications Engineer. July 6, 2007.
11. INFOCHEM *MULTIFLASH, Version 3.7.05*. London, U.K; 2007.
12. Tsonopoulos C. Thermodynamic analysis of the mutual solubities of normal alkanes and water. *Fluid Phase Equilibria*. 1999;156: 21–33.
13. Birch KP, Downs MJ, Ward RE. The measurements of humidity variations in gases resulting from the adsorption of water on to surfaces. *J Phys E Sci Instrum.* 1988:692–694.

Manuscript received Sept. 12, 2008, revision received Dec. 13, 2008, and final revision received Feb. 10, 2009.